J Bioenerg Biomembr (2015) 47:431–440
DOI 10.1007/s10863-015-9622-z

A novel viral thymidylate kinase with dual kinase activity

Eduardo Guevara-Hernandez[1,2] · Aldo A. Arvizu-Flores[3] · Maria E. Lugo-Sanchez[1] · Enrique F. Velazquez-Contreras[3] · Francisco J. Castillo-Yañez[3] · Luis G. Brieba[4] · Rogerio R. Sotelo-Mundo[1]

Received: 25 March 2015 / Accepted: 17 August 2015 / Published online: 28 August 2015
© Springer Science+Business Media New York 2015

Abstract Nucleotide phosphorylation is a key step in DNA replication and viral infections, since suitable levels of nucleotide triphosphates pool are required for this process. Deoxythymidine monophosphate (dTMP) is produced either by de novo or salvage pathways, which is further phosphorylated to deoxythymidine triphosphate (dTTP). Thymidyne monophosphate kinase (TMK) is the enzyme in the junction of both pathways, which phosphorylates dTMP to yield deoxythymidine diphosphate (dTDP) using adenosine triphosphate (ATP) as a phosphate donor. White spot syndrome virus (WSSV) genome contains an open reading frame (ORF454) that encodes a thymidine kinase and TMK domains in a single polypeptide. We overexpressed the TMK ORF454 domain (TMKwssv) and its specific activity was measured with dTMP and dTDP as phosphate acceptors. We found that TMKwssv can phosphorylate dTMP to yield dTDP and also is able to use dTDP as a substrate to produce dTTP. Kinetic parameters K_M and k_{cat} were calculated for dTMP (110 μM, 3.6 s^{-1}), dTDP (251 μM, 0.9 s^{-1}) and ATP (92 μM, 3.2 s^{-1}) substrates, and TMKwssv showed a sequential ordered bi-bi reaction mechanism. The binding constants K_d for dTMP (1.9 μM) and dTDP (10 μM) to TMKwssv were determined by Isothermal Titration Calorimetry. The affinity of the nucleotidic analog stavudine monophosphate was in the same order of magnitude (K_d 3.6 μM) to the canonical substrate dTMP. These results suggest that nucleotide analogues such as stavudine could be a suitable antiviral strategy for the WSSV-associated disease.

Keywords Thymidylate kinase · Nucleotide phosphorylation · Diphosphate kinase · Isothermal titration calorimetry · White spot syndrome virus

Electronic supplementary material The online version of this article (doi:10.1007/s10863-015-9622-z) contains supplementary material, which is available to authorized users.

✉ Aldo A. Arvizu-Flores
aldoarvizu@guayacan.uson.mx

✉ Rogerio R. Sotelo-Mundo
rrs@ciad.mx

[1] Centro de Investigación en Alimentación y Desarrollo, A.C. (CIAD), Carretera a Ejido La Victoria Km 0.6, Apartado Postal 1735, Hermosillo, Sonora 83304, Mexico

[2] Departamento de Investigación y Posgrado en Alimentos, Universidad de Sonora, Blvd. Rosales y Luis Encinas, Hermosillo, Sonora 83000, Mexico

[3] Departamento de Ciencias Químico Biológicas, Universidad de Sonora, Blvd. Rosales y Luis Encinas, Hermosillo, Sonora 83000, Mexico

[4] Laboratorio Nacional de Genómica para la Biodiversidad (LANGEBIO), Centro de Investigación y Estudios Avanzados-Unidad Irapuato, Km 9.6 Libramiento Norte Carretera Irapuato-León, Apartado Postal 629, Irapuato, Guanajuato 36500, Mexico

Introduction

Pathogens have developed strategies to provide and maintain their nucleotides pool. The White Spot Syndrome Virus (WSSV), which affects marine invertebrates, contains a double stranded circular DNA genome of about 300 kbp that encodes several enzymes involved in DNA metabolism (van Hulten et al. 2001). Some of those genes characterized to date include a DNA polymerase (de-la-Re-Vega et al. 2011), a ribonucleotide reductase (van Hulten et al. 2000), a thymidylate synthase (Arvizu-Flores et al. 2009) and a bifunctional polypeptide with thymidine kinase (TK) and thymidine monophosphate

kinase (TMK) domains (Guevara-Hernandez et al. 2012; Tsai et al. 2000). The TK-TMK arrangement as a duplicated gene present in WSSV is unique in all kinases currently studied.

Other viral TMKs recently studied include variola virus (Guimarães et al. 2014), *Epinopia aporema* granulovirus (Ferrelli et al. 2012), vaccinia poxvirus (Caillat et al. 2008), Chilo iridescent virus (Jakob et al. 2001) and one recently identified in *Erwinia* phage Ea35-70 (GenBank entry AHI60461.1) (Yagubi et al. 2014). These and other studies highlighted viral TMKs as a target against viral diseases, because of its role in the de novo and salvage pathways for deoxythymidine triphosphate (dTTP) synthesis. dTTP formation is catalyzed by three different kinase proteins: TK, TMK and the nonspecific-nucleotide diphosphate kinase (NDK). In crustaceans like *Litopenaeus vannamei*, which is the WSSV host, the third phosphorylation step for dTTP is catalyzed by NDK (Quintero-Reyes et al. 2012; Ghaffari et al. 2014).

In a previous work, we found that the TMK domain of WSSV ORF454 (TMKwssv) is a functional enzyme by itself, with ATP-dependent phosphorylation of deoxythymidine monophosphate (dTMP) to produce deoxythymidine diphosphate (dTDP) (Guevara-Hernandez et al. 2012). In the present work, we observed that TMKwssv is able to catalyze the ATP-dependent phosphorylation of dTDP to produce dTTP. Therefore, the thymidine nucleoside (dT) could be phosphorylated to dTTP solely by the WSSV ORF454 gene product. Two sequential phosphorylation reactions catalyzed by one single polypeptide have been observed in dual viral thymidine kinases, from human herpes virus TK (HSV-1) (Chen and Prusoff 1978) and equine herpes virus TK (Gardberg et al. 2003). Therefore, the objective of this work was to study the kinetic and thermodynamic properties of TMKwssv. Since this virus also encodes its own thymidylate synthase, we envision that the virus provides its own dTTP for viral DNA replication.

Experimental procedures

Reagents

Radiolabeled [γ-P^{32}] ATP was purchased from Perkin-Elmer, thin layer sheets were from Merck-Millipore, adenosine 5′-(β,γ-imino) triphosphate (AMP-PNP) was from Roche. Stavudine monophosphate (2′,3′-didehydro-2′,3′-dideoxy-thymidine-5′-monophosphate, d4TMP) was from Jenna Bioscience. Pyruvate kinase, lactate dehydrogenase, buffers, salts, reagents for microbiology and general chemicals were acquired from Sigma-Aldrich.

TMK expression and purification

TMKwssv was purified as reported (Guevara-Hernandez et al. 2012) from recombinant bacterial expression of a synthetic construct containing the TMK domain (residues 201 to 398) from the TK-TMK from WSSV (GenBank: NP_477917).

Thin layer chromatography

TLC was used to determine specific thymidine monophosphate kinase activity (Neuhard et al. 1965; Van Rompay et al. 1999; Yegutkin et al. 2001). The reaction buffer contained 50 mM Tris–HCl pH 7.5, 2 mM $MgCl_2$, 0.2 mM dTMP, 0.5 mg/mL BSA, 1 mM DTT, and 15 mM NaF. The reaction was started by addition of 1 μCi of [γ-P^{32}]ATP and 40 ng of TMKwssv in a final reaction volume of 20 μL. Samples of the reaction were stopped at 2, 4, 8 and 16 min by heating at 70 °C for 2 min. Aliquots of 2 μl for each sample were spotted onto a TLC PEI cellulose 20×20 cm sheet (Merck Millipore) and samples were eluted inside a TLC chamber with 0.5 M ammonium formate pH 3.5. Samples were visualized with a phosphorimager and analyzed with the Quantity-One software (BioRad).

High-performance liquid chromatography

The dual kinase activity of TMKwssv was determined using an HPLC system and UV cell detector series 1100 (Agilent Technologies). Detection of dTTP formation was followed as described for nucleotide separation (Ryder 1985) and with modifications (Marquez-Rios et al. 2007). Reactions were performed in 25 mM Tris HCl pH 7.4, 150 mM NaCl, 5 mM $MgCl_2$, 1 mM ATP and 1 mM dTDP, and were started by adding 50 μg of TMKwssv in a final volume of 1 mL, at 25 °C and 100 rpm of orbital agitation. Reactions were stopped by addition of 0.6 M perchloric acid at 1, 2 and 3 h. Each sample was centrifuged at 16,000×*g* for 30 min at 4 °C, neutralized with 1 M of KOH solution and filtered through a 0.22 μm membrane. Aliquots of 20 μL were injected in a reverse-phase column Ultrasphere 4.6 mm×250 mm and 5 μm of particle size (Beckman Coulter) using potassium phosphate 0.1 M buffer pH 7.0 as a mobile phase at a 2.5 mL/min flow rate. Run was performed isocratically for 20 min at 30 °C and eluent was monitored at 254 nm. Quantification was made by a standard curve, fitted in a linear regression model made with different nucleotides standard concentrations.

Enzyme kinetics

TMK activity was determined in a coupled enzymatic assay following NADH oxidation dependent of ADP formation at

37 °C (Blondin et al. 1994; Guevara-Hernandez et al. 2012; Topalis et al. 2005). The reaction mixture in a final volume of 1 mL contained 50 mM Tris–HCl pH 7.4, 50 mM KCl, 5 mM $MgCl_2$, 0.2 mM NADH, 1 mM phosphoenol pyruvate, 1 mM DTT, 4 U of pyruvate kinase and 4 U of lactate dehydrogenase. Substrates ATP, dTMP and dTDP were used at several concentrations between 0.005 and 2 mM. The coupled assay was initiated by the addition of 5 μg of TMKwssv to the reaction mixture and NADH oxidation was followed for 200 s at 340 nm. Initial rates were expressed as $\mu mol \cdot s^{-1}$ and data were fitted to a Michaelis-Menten kinetic model whit GraphPad Prism 6 software. All runs were made by triplicate.

Isothermal titration calorimetry

Nucleotide binding was performed on a VP-ITC microcalorimeter (Microcal, GE Healthcare Life Sciences). The TMKwssv solution was dialyzed overnight with 25 mM Tris–HCl pH 7.4, 150 mM NaCl, 5 mM $MgCl_2$ and 10 % ethylene glycol. Ligand syringe concentrations were 0.6 mM for ATP, 0.8 mM for dTMP and dTDP, and 0.4 mM for d4TMP, all solutions were prepared with final dialysis buffer. Sample cell (1.4 mL) was filled with 1 mg/mL TMKwssv solution and reference cell was filled with final dialysis buffer solution. The titrations were run with 30 injections of 8 μL at 25 °C and 199 rpm. Binding experiments for thymidine nucleotides were made in absence and presence of AMP-PNP as a non-hydrolyzable ATP analog (Petit and Koretke 2002). Data were fitted using Microcal Origin software to yield dissociation constant (K_d), enthalpy (ΔH) and entropy (ΔS) values.

Molecular docking

Computational docking was used to predict dTDP and d4TMP binding to the active site of TMKwssv using the MOE v2013.10 software (Chemical Computing Group). A TMKwssv molecular model was previously built based on the homology to human TMK crystal structure reported in PDB: 1E9C (Ostermann et al. 2003), which included AMP-PNP and dTMP ligand coordinates within active site of TMKwssv. A conformer database was generated for each ligand dTMP, dTDP and d4TMP. The docking site was defined as the dTMP binding site plus AMP-PNP and Mg^{2+}. Three independent stochastic runs were performed to gain convergence of the best scoring positions; also, we used dTMP as a ligand to verify the accuracy of predicted poses. The induced fit protocol was used to sample 60,000 poses for each conformer using the alpha triangle placement methodology. According to the default scoring function of MOE, the best 30 poses for each ligand were retained for a posterior structural refinement using the force field method for the energy minimization steps. The 30 top scoring poses selected with the ΔG affinity function were analyzed.

Results

The monophosphate kinase activity of the recombinant TMKwssv domain was reported previously (Guevara-Hernandez et al. 2012). To further characterize the TMKwssv activity by a direct method, we used a radioactive assay for thymidine monophosphate kinase activity (Neuhard et al. 1965; Van Rompay et al. 1999) and a HPLC strategy to identify dTTP formation from thymidine diphosphate kinase activity (Ryder 1985). Furthermore, the findings from the dual activity of TMKwssv were also analyzed by enzyme kinetics on a coupled assay, binding experiments from ITC and in silico docking.

Identification of the TMKwssv dual kinase activity

The formation of dTDP was confirmed with a radioactive assay using [γ-P^{32}]ATP and TLC. In Fig. 1, the appearance of a spot from [β-P^{32}]dTDP was dependent on the addition of TMKwssv to the reaction mixture. However, formation of [β-P^{32}]dTDP was not detected in the absence of the enzyme or in the presence of an unrelated protein.

Some kinases are able to phosphorylate subsequent steps in a nucleotide phosphorylation pathway or are able to phosphorylate different nucleotides (Chen and Prusoff 1978; Gardberg et al. 2003; Motomura et al. 2014; Perozzo et al. 2000). Considering this, we probed specific kinase activity on the coupled enzymatic assay using dT, dUMP and dTDP as a phosphate acceptors. We only observed kinase activity using dTMP (the cognate substrate) and with dTDP, whereas for dT and dUMP the kinase activity was negligible (data no shown). Additional confirmation of this dual kinase activity was obtained by HPLC to confirm dTTP formation (Ryder 1985). In this technique, different nucleotides are separated based on their different retention times on a reverse phase column (Fig. 2) in an endpoint assay.

Compared to the blank reaction (dotted line), the addition of TMKwssv resulted in the appearance of ADP and dTTP peaks (continuous line) and consumption of ATP and dTDP.

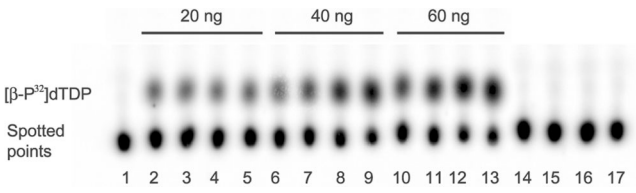

Fig. 1 [β-P^{32}]dTDP formation by TMKwssv. TLC of TMKwssv + dTMP + ATP reaction. Lane 1, blank reaction with no enzyme. Lanes 2–5, reactions with 20 ng of TMKwssv stopped at 2, 4, 8 and 16 min. Lanes 6–9, reactions with 40 ng of TMKwssv stopped at 2, 4, 8 and 16 min. Lanes 10–13, reactions with 60 ng of TMKwssv stopped at 2, 4, 8 and 16 min. Lanes 14–17 contained 100 ng of *E. histolytica* PCNA at the same times as controls

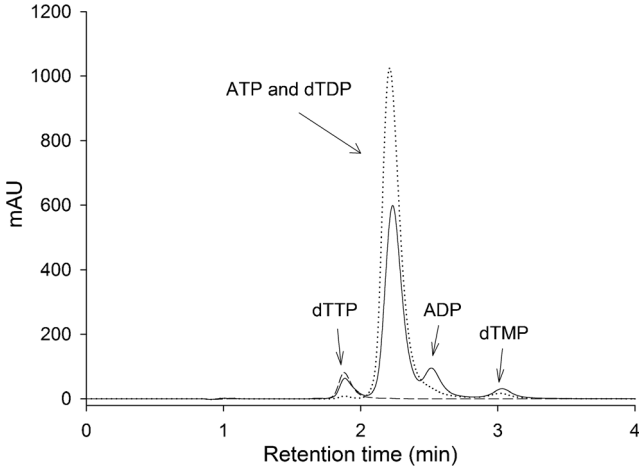

Fig. 2 dTTP formation by TMKwssv. HPLC chromatogram of TMKwssv + dTDP + ATP after 3 h of reaction. *Continuous line*: TMKwssv after 3 h of reaction with all reagents. *Dashed line*: dTTP standard. *Dotted line*: blank reaction without enzyme after 3 h

Formation of dTTP was confirmed by comparison to a dTTP standard (discontinuous line).

Kinetics parameters of TMKwssv

To further address the use of nucleotidic substrates, the steady-state kinetic parameters for TMKwssv were determined using a coupled assay for dTMP and dTDP.

The K_M for dTMP was 110±14 μM and for the phosphate-donor ATP was 92±8.5 μM (Fig. 3, panel a). The enzyme also was able to use dTDP as a substrate (Fig. 3, panel b), but showed less affinity compared to dTMP, with a K_M of 251±22 μM. Also, the K_M for ATP was raised to 224±33 μM when using dTDP as substrate. Since ATP and dTDP K_M increased, this suggests an ordered sequential mechanism, because a random sequential mechanism predicts that K_M for ATP would not change (Segel 1976). The turnover number k_{cat} was 3.56± 0.12 s^{-1} for dTMP, 3.16±0.062 s^{-1} for ATP, and 0.8924 ±0.023 s^{-1} for dTDP (Table 1). TMKwssv showed less affinity towards dTMP and the smallest catalytic efficiency in contrast to other reported TMK enzymes.

Non specific NDKs have K_M values in the sub mili molar range, like in spinach (Zhang et al. 1995), viral TMK (Topalis et al. 2005) or in TMKwssv using dTDP as substrate.

Lineweaver-Burk plots for ATP-dependent dTMP phosphorylation were indicative of a sequential binding mechanism (Fig. 4) in which dTMP binds first. The same was observed for dTDP phosphorylation reaction catalyzed by TMKwssv. This ordered binding could explain the rise in K_M value for ATP when using dTDP as the phosphate acceptor.

Thymidine nucleotides binding to TMKwssv

Binding of thymidine nucleotides to TMKwssv was measured by ITC. First, binary complex formation was analyzed using dTMP or ATP as ligands with the enzyme. Dissociation constants K_d and thermodynamic parameters were determined (Table 2).

TMKwssv was able to bind dTMP (Fig. 5 panel a) but not ATP alone (Fig. 5 panel b), which is in agreement to the ordered binding mechanism suggested by the enzyme kinetic analysis, requiring nucleotide binding before the phosphate donor could bind the active site. dTMP binding was adjusted to a sequential model with two sites with dissociation constants of 1.9 and 27 μM (Table 2). Interestingly, dTMP binding for TMKwssv was endothermic so it was for the non-hydrolyzable analog ATP[S] in *S. pneumonia* TMK (Petit and Koretke 2002). For the latter, dTMP was bound after the phosphate donor and the binding was exothermic. Since all are nucleotides, it appears that the first ligand binds endothermally, implying that there is an important conformational change involved (Li de la Sierra et al. 2001).

As we had evidence of the dual activity of TMKwssv, we determined the dissociation constant for dTDP and d4TMP in the presence of AMP-PNP (Fig. 6). d4TMP is the phosphorylated form of stavudine (d4T), as it would be produced by thymidine kinase, either from the same virus or from the host.

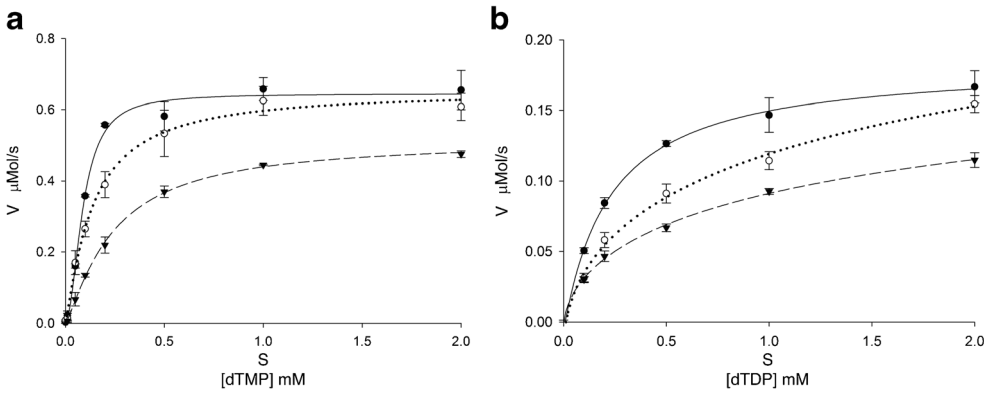

Fig. 3 Kinetic analysis for TMKwssv. **a** Michaelis-Menten kinetics for different concentrations of dTMP (Panel **a**) and dTDP (Panel **b**), at three different ATP concentrations: *continuous line* 1 mM, *dotted line* 0.5 mM, *dashed line* 0.2 mM

Table 1 Comparison of kinetic parameters of different TMK. K_M and k_{cat} determination for TMKwssv was at 37 °C by coupled enzymatic assay

Organism	K_M (μM)			k_{cat}/K_M (s^{-1} mM^{-1})		
	ATP	dTMP	dTDP	ATP	dTMP	dTDP
WSSV (This work)	92±8.5	110±14	251±22	34	32	4
Vaccinia virus (Topalis et al. 2005)	130	20		16	100	
E. coli (Lavie et al. 1998)	8	3		1875	5600	
M. tuberculosis (Munier-Lehmann et al. 2001)	100	40		45	1000	
H. sapiens (Ostermann et al. 2000)	5	5		140	140	
S. cerevisiae (Lavie et al. 1998)	190	9		184	3900	
P. falciparum (Whittingham et al. 2010)	79	11		62	460	
B. malayi (Doharey et al. 2014)	66	17		577	2240	
S. pneumonia (Petit and Koretke 2002)	235	66		38	134	

Since this compound lacks the 2′ and 3′-hydroxyl groups for the nucleoside ribose, it is a substrate with the capacity of being an antiviral compound as a chain termination for viral DNA polymerase. d4T has been used as an antiviral drug and it should bind to the TMKwssv active site in its monophosphorylated form.

The K_d values for dTDP were 10 and 215 μM, about five times the value for dTMP. The K_{d1} constant is similar to the K_d of 13.7 μM for white shrimp (*Litopenaeus vannamei*) NDK (Quintero-Reyes et al. 2012) and 1.4 μM for the *P. falciparum* NDK (Kandeel and Kitade 2010). The K_d value for d4TMP was 3.6 μM, similar to the cognate substrate dTMP. It was remarkable that two compounds with almost identical structure, one lacking the sugar 3′-OH compared to the cognate substrate, had the same affinity.

As proposed by Freire (Freire 2008), a graph describing the thermodynamic values is helpful in understanding the binding process. The thermodynamic signatures of the nucleotide binding process are presented in Fig. 7.

Molecular modeling and docking

To propose a model for TMKwssv nucleotide binding, a structural docking was realized with dTMP, d4TMP and dTDP. The TMKwssv theoretical model (Guevara-Hernandez et al. 2012) was used as template model in which relevant catalytic loops P-loop, lid-loop and DRY-loop were identified (Ostermann et al. 2000). Docking of dTMP to its binding site was achieved in almost the same position as the coordinates previously predicted for the theoretical ternary complex of TMKwssv modeled from the template coordinates (Fig. 8).

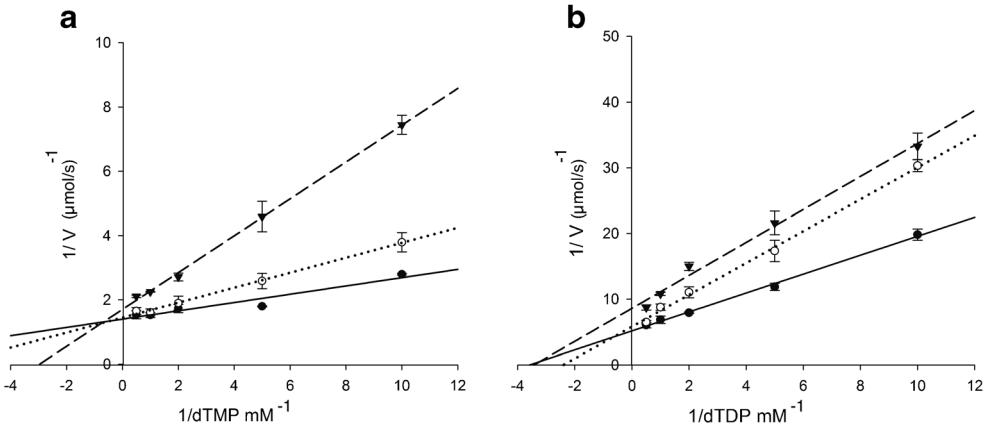

Fig. 4 Lineweaver-Burk plots for TMKwssv. Double reciprocal plots at different concentrations of dTMP and dTDP were plotted at three different concentration of ATP: *continuous line* 1 mM, *dotted line* 0.5 mM, *dashed line* 0.2 mM. For bi-substrate enzymes, intersections of plotted lines suggest a sequential reaction mechanism

Table 2 Dissociation constants and thermodynamic parameters for nucleotide binding to TMKwssv. Binding to dTMP and dTDP was sequential and therefore two dissociation constants and two set of parameters were determined. Stavudine monophosphate (d4TMP) binding was modeled to a single site. Dilution heat was subtracted before calculations

Nucleotide	K_{d1} (μM)	K_{d2} (μM)	Δ H1 cal/mol	Δ H2 cal/mol	Δ S1 cal/mol/deg	Δ S2 cal/mol/deg
dTMP	1.9	27	-1.38×10^4	-4.5×10^3	−20.4	5.7
dTDP	10	215	-1.22×10^4	1.9×10^2	−18.2	
d4TMP	3.6		-1.77×10^4		−34.7	17.4
ATP	n.d.					

We found that the ribose 3′-OH of dTMP could make a hydrogen bond with Glu150 and the sugar ring match the expected position. Also, the thymidine nucleobase is well positioned inside the hydrophobic pocket as observed in crystallographic structures of other TMK. The main differences between several poses obtained from this docking regards to the position of the phosphate group, that shifts outside the catalytic site.

As we have shown that TMKwssv can bind and phosphorylate dTDP, we docked this molecule into the TMKwssv active site theoretical model. Figure 9 shows the predicted positions where the diphosphate nucleotides are positioned compared to the dTMP coordinates. The computational model proposes a hydrogen bond between the dTMP 3′-OH of the ribose sugar ring and Glu150 from the lid loop, similar to the prediction with dTMP. In the crystal structure of human TMK, the sugar dTMP 3′-OH forms a hydrogen bond with an acidic residue (Asp15) from the P-loop in the closed conformation. Such difference makes clear the need of a crystal structure of the novel TMKwssv.

With respect to d4TMP (Fig. 10), with all the reserves of a theoretical structural model, the position of the dideoxy nucleotide is slightly displaced, leaving space for an ordered water molecule that could satisfy the hydrogen bonding of the acidic group and be consistent with the experimental thermodynamical data.

Discussion

During the WSSV viral infection, the ORF454 that encodes TMKwssv is expressed early during the disease (Liu et al.

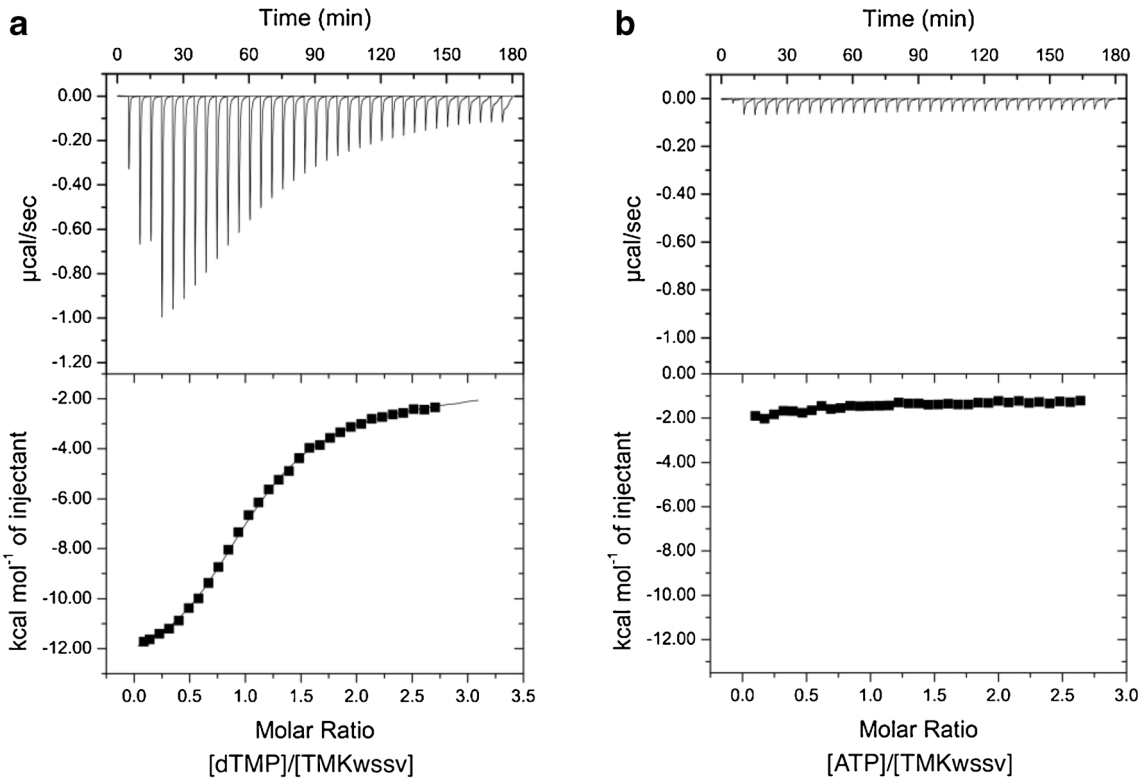

Fig. 5 Binding thermograms for dTMP and ATP. **a** dTMP titration, **b** ATP titration, no binding heat was detected

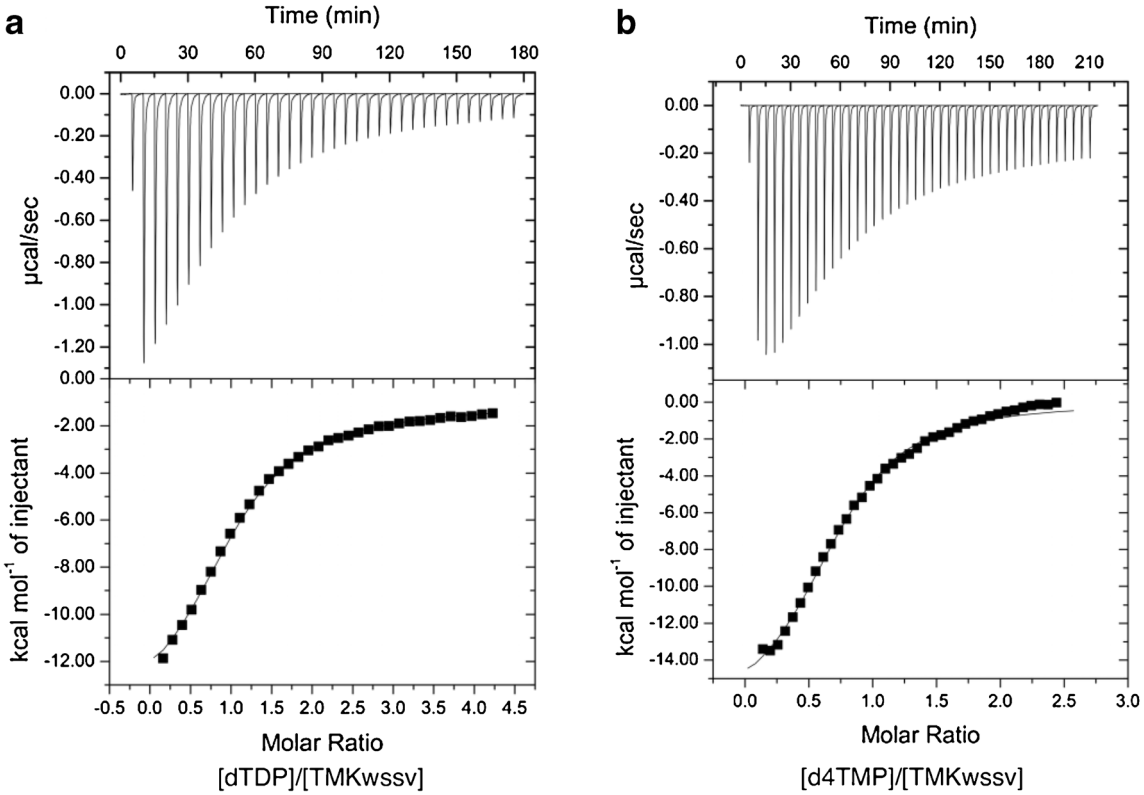

Fig. 6 Binding thermograms for dTDP and d4TMP in ternary complex with AMP-PNP. **a** dTDP titration, **b** d4TMP titration

2005). If the polypeptide is expressed and processed into separate polypeptides, the TKwssv domain would perform the salvage pathway and viral thymidylate synthase (Arvizu-Flores et al. 2009) and TMKwssv with its dual kinase activity would complete the de novo dTTP synthesis pathway.

For this novel dual kinase, we propose that a kinetic ordered sequential mechanism occurs, where TMKwssv binds first the phosphate acceptor (dTMP or dTDP) and later the phosphate donor (ATP). The formation of a strong binary complex (dTMP-TMKwssv), no apparent phosphate donor binding, and enzyme kinetic, support a model where dTMP-TMKwssv binary complex is preformed before ATP could bind. Other TMKs showed different sequential binding schemes. For example, in the mechanism reported for *Streptococcus pneumoniae* TMK, dTMP binds after the binary complex TMK-ATP is formed (Petit and Koretke 2002). For mouse and human TMK, the reaction mechanism described was random bi bi, as suggested from crystallographic studies, as well as reported for homolog proteins guanylate and adenylate kinases (Cheng and Prusoff 1973; Ostermann et al. 2000). Other evidence came from ITC, where we observed that TMKwssv could bind dT (data not shown)

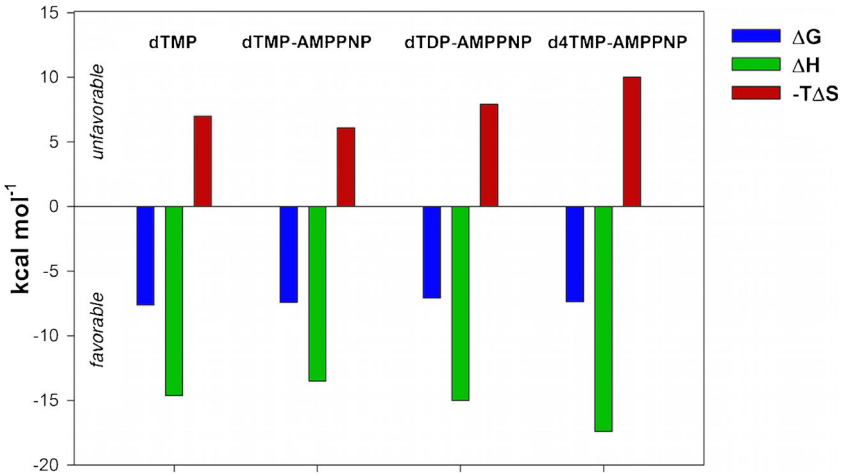

Fig. 7 Thermodynamic signature of TMKwssv. Thermodynamics parameters of TMKwssv with ligands: dTMP, dTMP-AMPPNP, dTDP-AMPPNP, d4TMP-AMPPNP at 25 °C

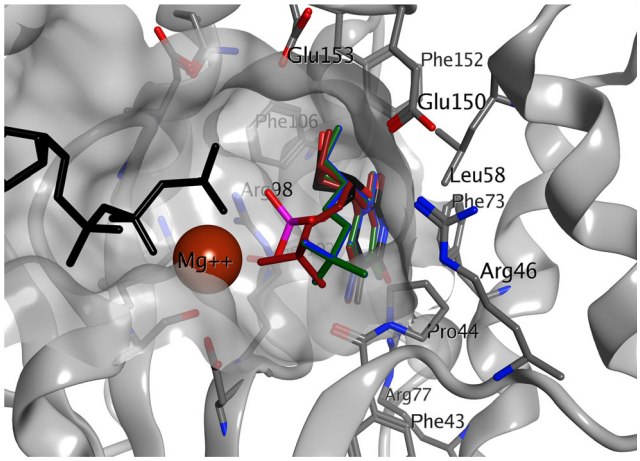

Fig. 8 Docking of dTMP into TMKwssv active site. In silico model of dTMP docked in the active site of TMKwssv. The best three poses of the nucleotide are overlapped. Mg^{++} is shown as a sphere and ATP in *black*. The side chains interacting with dTMP are colored and labeled

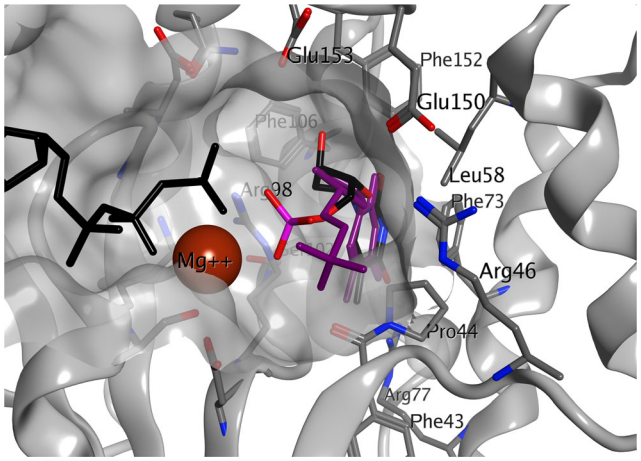

Fig. 10 Docking of d4TMP into TMKwssv active site. In silico model of stavudine monophosphate (d4TMP) docked in the active site of TMKwssv. The best three poses of the nucleotide are overlapped. Mg^{++} is shown as a sphere and ATP in *black*. The side chains interacting with dTMP are colored and labeled

forming a similar binary complex to dTMP. However, this binary complex did not show the formation of ternary complex with ATP, nor specific TK activity, possibly because the phosphate of dTMP is necessary for the proper binding of ATP or active site closure.

Using a simple bar graph displaying the thermodynamical parameters, it is possible to make an "energetics signature graph" (Fig. 7), that could be easily visualized and compared between ligands (Freire 2008; Kawasaki and Freire 2011). Binding of thymidine nucleotides was highly exothermic with a negative enthalpy change (ΔH), corresponding to strong hydrogen bonds to the phosphate groups (Kandeel and Kitade 2010). The entropic component -TΔS in all cases was unfavorable, which implies that more water molecules are ordered upon nucleotide binding (Fig. 7). However, the unfavorable entropic contribution is compensated by the larger enthalpic component due to hydrogen bonding, leading to a negative ΔG. The crystal structure of human TMK shows that the lid loop has large movements towards the nucleotide substrate (Ostermann et al. 2000).

Comparative analysis of d4TMP and dTMP is critical because both molecules differ in one hydroxyl group of the nucleotide ribose ring. Although their ΔG (−7.68 vs. −7.42 kcal/mol) and hence their K_d values are very similar, the entropic components (10.02 vs. 6.08 kcal/mol) differ by about 4 kcal/mol or one hydrogen bond (Freire 2008). Interestingly, the crystal structure of shrimp NDK bound to a ribo or deoxynucleotide differs by hydrogen bond satisfied by an ordered water molecule (Lopez-Zavala et al. 2014).

With respect to the diphosphate substrate (dTDP) vs. the cognate (dTMP), the energetics are more subtle. Dissociation constants are almost identical (6.25 vs. 3.28 μM) and the major difference is on the enthalpic ΔG component (−15.0 vs. −13.5 kcal/mol). Quantitatively the difference (1.5 kcal/mol) does not account for a hydrogen bond but qualitatively reflects that the diphosphate nucleotide makes more hydrogen bonds by having and additional phosphate group.

For dTDP, the docking proposed the formation of a hydrogen bond with 3′-OH from the nucleotide. Both phosphates from dTDP are accommodated in place with the active site and magnesium ion suitable for the phosphate transfer reaction, according to the crystallographic structures (Ostermann et al. 2000). However, the phosphate changed its position in the different poses, despite that the sugar ribose and thymine base are very well located and proper hydrophobic contacts are made with the binding site residues. Similar results were observed in the crystallographic structure of dual TK from HSV-1, where the position of the phosphates in TP5A (P^1-(5′-adenosyl) P^5-[5′-(2′-deoxy-thymidyl)] tetraphosphate) ligand shifts between distinct poses (Gardberg et al. 2003).

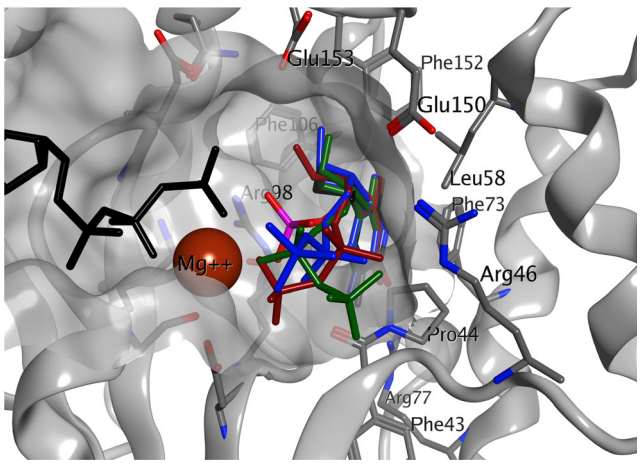

Fig. 9 Docking of dTDP into TMKwssv active site. In silico model of dTDP docked in the active site of TMKwssv. The best three poses of the nucleotide are overlapped. Mg^{++} is shown as a sphere and ATP in *black*. The side chains interacting with dTMP are colored and labeled

This suggests that TMKwssv could bind dTDP in a shifted position proper for phosphate transfer from ATP.

Conclusions

Unlike other TMK previously reported (Cheng and Prusoff 1973; Doharey et al. 2014; Guimarães et al. 2014; Kandeel and Kitade 2011; Kandeel et al. 2014; Lavie and Konrad 2004; Topalis et al. 2005), to our knowledge TMKwssv is the first TMK reported able to bind dTDP as a phosphate acceptor. This interaction was observed in human TMK-dTDP complexes with ADP in crystal structure, where the authors assumed that the complex is formed in reaction sense direction, i.e. just before the release of product (Ostermann et al. 2000). Other viral kinases were able to perform sequential phosphorylation steps, like the HSV-1 TK. This kinase only interacts with ATP when phosphate receptor (thymidine) are in complex with the kinase, and also is able to perform the next phosphorylation step in which dTMP are the phosphate receptor to yield dTDP (Perozzo et al. 2000).

Kinetic and thermodynamic assays showed about two-orders of magnitude between dissociation (K_d) and Michaelis kinetic (K_M) constants. For example, K_d for dTMP and dTDP affinities were 3.28 and 6.25 μM respectively; whereas K_M for dTMP was 110 and 251 μM for dTDP. As additional experimental evidence, we determined the presence of dTTP by HPLC using only dTMP substrate. Based on these results we propose that the double phosphorylation of dTMP to yield dTTP does not occur simultaneously. This data suggests that dTMP is used in first place as phosphate receptor; then, dTDP is used but only when dTMP is exhausted.

Thymidine metabolism is key for DNA replication. It is remarkable that the WSSV genome encodes a protein that involves both de novo and salvage nucleotide pathways. The thymidine kinase activity has been reported (Tzeng et al. 2002) and now we show that the TMK domain is a functional dTMP/dTDP kinase.

Our results will help to establish treatment strategies with nucleotide analogs as antiviral compounds. Although it has not yet been demonstrated that the viral kinase TK-TMK gene product is processed in vivo leading to two separate functional polypeptides during viral infection, this work has shown that the TMK domain is biochemically and structurally feasible. Also, it is shown that the product of ORF454 of the WSSV bifunctional gene is capable of performing all three phosphorylation reactions necessary for the formation of dTTP.

Acknowledgments This work was supported by Mexico's Consejo Nacional de Ciencia y Tecnología (CONACYT) grants CB-2009-131859 to R. Sotelo-Mundo and INFR-2013-01-205617 to A. Arvizu-Flores for ITC equipment. E. Guevara-Hernandez received a graduate scholarship from CONACYT. We thank the following personnel from CIAD: Mr. Gerardo Reyna for bibliographical support and to Mr. Felipe Isac, Luis Leyva, Adalberto Murrieta, Jose Luis Aguilar and Martin Peralta for computational support.

References

Arvizu-Flores AA, Aispuro-Hernandez E, Garcia-Orozco KD, Varela-Romero A, Valenzuela-Soto E, Velazquez-Contreras EF, Rojo-Domínguez A, Yepiz-Plascencia G, Maley F, Sotelo-Mundo RR (2009) Comp Biochem Physiol Part C Toxicol Pharmacol 150: 406–413

Blondin C, Serina L, Wiesmuller L, Gilles A-M, Barzu O (1994) Anal Biochem 220:219–221

Caillat C, Topalis D, Agrofoglio LA, Pochet S, Balzarini J, Deville-Bonne D, Meyer P (2008) Proc Natl Acad Sci U S A 105:16900–16905

Chen MS, Prusoff WH (1978) J Biol Chem 253:1325–1327

Cheng Y-C, Prusoff WH (1973) Biochemistry 12:2612–2619

De-La-Re-Vega E, Garcia-Orozco KD, Arvizu-Flores AA, Yepiz-Plascencia G, Muhlia-Almazan A, Hernández J, Brieba LG, Sotelo-Mundo RR (2011) Molecules 16:532–542

Doharey PK, Suthar MK, Verma A, Kumar V, Yadav S, Balaramnavar VM, Rathaur S, Saxena AK, Siddiqi MI, Saxena JK (2014) Acta Trop 133:83–92

Ferrelli ML, Salvador R, Biedma ME, Berretta MF, Haase S, Sciocco-Cap A, Ghiringhelli PD, Romanowski V (2012) BMC Genomics 13:548

Freire E (2008) Drug Discov Today 13:869–874

Gardberg A, Shuvalova L, Monnerjahn C, Konrad M, Lavie A (2003) Structure 11:1265–1277

Ghaffari N, Sanchez-Flores A, Doan R, Garcia-Orozco KD, Chen PL, Ochoa-Leyva A, Lopez-Zavala AA, Carrasco JS, Hong C, Brieba LG, Rudino-Pinera E, Blood PD, Sawyer JE, Johnson CD, Dindot SV, Sotelo-Mundo RR, Criscitiello MF (2014) Sci Rep 4:7081

Guevara-Hernandez E, Garcia-Orozco KD, Sotelo-Mundo R (2012) Protein Pept Lett 19:1220–1224

Guimarães AP, Ramalho TC, França TCC (2014) J Biomol Struct Dyn 32:1601–1612

Jakob NJ, Muller K, Bahr U, Darai G (2001) Virology 286:182–196

Kandeel M, Kitade Y (2010) J Bioenerg Biomembr 42:361–369

Kandeel M, Kitade Y (2011) Biol Pharm Bull 34:173–176

Kandeel M, Noguchi Y, Oh-Hashi K, Kim H-S, Kitade Y (2014) J Therm Anal Calorim 115:2089–2097

Kawasaki Y, Freire E (2011) Drug Discov Today 16:985–990

Lavie A, Konrad M (2004) Mini Rev Med Chem 4:351–359

Lavie A, Ostermann N, Brundiers R, Goody RS, Reinstein J, Konrad M, Schlichting I (1998) Proc Natl Acad Sci 95:14045–14050

Li De La Sierra I, Munier-Lehmann H, Gilles AM, Barzu O, Delarue M (2001) J Mol Biol 311:87–100

Liu WJ, Chang YS, Wang CH, Kou GH, Lo CF (2005) Virology 334: 327–341

Lopez-Zavala AA, Quintero-Reyes IE, Carrasco-Miranda JS, Stojanoff V, Weichsel A, Rudino-Pinera E, Sotelo-Mundo RR (2014) Acta Crystallogr Sect F Struct Biol Cryst Commun 70:1150–1154

Marquez-Rios E, Moran-Palacio EF, Lugo-Sanchez ME, Ocano-Higuera VM, Pacheco-Aguilar R (2007) J Food Sci 72:C356–C362

Motomura K, Hirota R, Okada M, Ikeda T, Ishida T, Kuroda A (2014) Appl Environ Microbiol 80:2602–2608

Munier-Lehmann H, Chaffotte A, Pochet S, Labesse G (2001) Protein Sci 10:1195–1205

Neuhard J, Randerath E, Randerath K (1965) Anal Biochem 13:211–222

Ostermann N, Schlichting I, Brundiers R, Konrad M, Reinstein J, Veit T, Goody RS, Lavie A (2000) Structure 8:629–642
Ostermann N, Segura-Peña D, Meier C, Veit T, Monnerjahn C, Konrad M, Lavie A (2003) Biochemistry 42:2568–2577
Perozzo R, Jelesarov I, Bosshard HR, Folkers G, Scapozza L (2000) J Biol Chem 275:16139
Petit C, Koretke K (2002) Biochem J 363:825–831
Quintero-Reyes IE, Garcia-Orozco KD, Sugich-Miranda R, Arvizu-Flores AA, Velazquez-Contreras EF, Castillo-Yanez FJ, Sotelo-Mundo RR (2012) J Bioenerg Biomembr 44:325–331
Ryder JM (1985) J Agric Food Chem 33:678–680
Segel IH (1976) Biochemical calculations: how to solve mathematical problems in general biochemistry. Wiley, New York
Topalis D, Collinet B, Gasse C, Dugué L, Balzarini J, Pochet S, Deville-Bonne D (2005) FEBS J 272:6254
Tsai ME, Yu HT, Tzeng HF, Jl-Leu CM, Chou CJ, Huang CH, Huang JY, Lin GH (2000) Virology 277:100–110
Tzeng HF, Chang ZF, Peng SE, Wang CH, Lin JY, Kou GH, Lo CF (2002) Virology 299:248–255
Van Hulten MCW, Tsai MF, Schipper CA, Lo CF, Kou GH, Vlak JM (2000) J Gen Virol 81:307
Van Hulten MCW, Witteveldt J, Peters S, Kloosterboer N, Tarchini R, Fiers M, Sandbrink H, Lankhorst RK, Vlak JM (2001) Virology 286:7–22
Van Rompay AR, Johansson M, Karlsson A (1999) Mol Pharmacol 56: 562–569
Whittingham J, Carrero-Lerida J, Brannigan J, Ruiz-Perez L, Silva A, Fogg M, Wilkinson A, Gilbert I, Wilson K, Gonzalez-Pacanowska D (2010) Biochem J 428:499–509
Yagubi AI, Castle AJ, Kropinski AM, Banks TW, Svircev AM (2014) Genome Announc 22:e00413–14
Yegutkin GG, Henttinen T, Jalkanen S (2001) FASEB J 15:251–260
Zhang J, Fukui T, Ichikawa A (1995) Biochim Biophys Acta 1248: 19–26